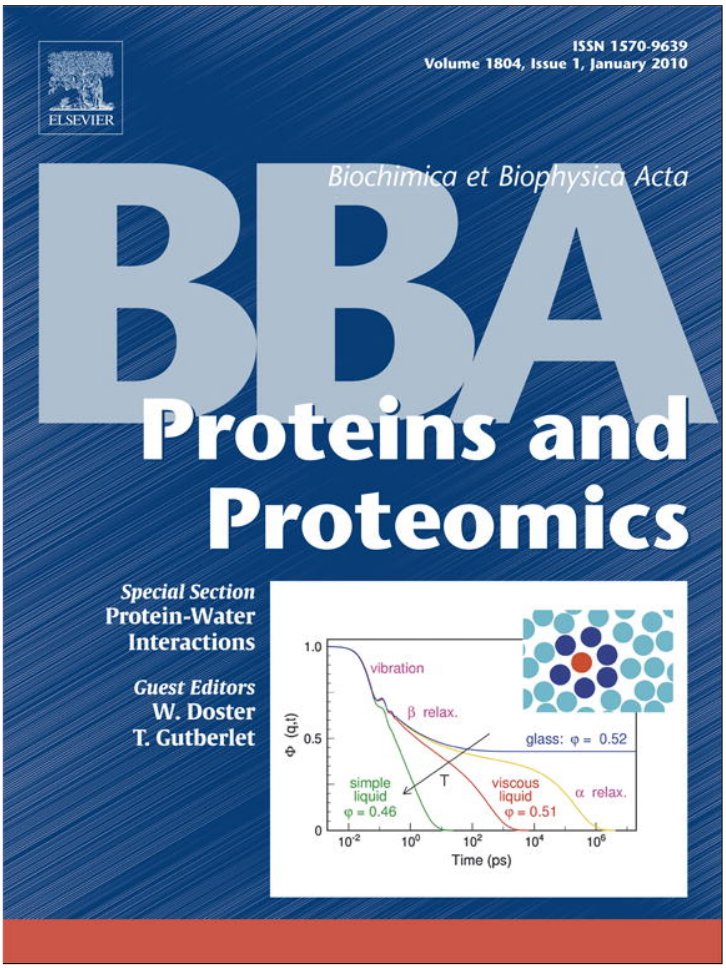

Biochimica et Biophysica Acta 1804 (2010) 3–14

Contents lists available at ScienceDirect

Biochimica et Biophysica Acta

journal homepage: www.elsevier.com/locate/bbapap

Review

The protein-solvent glass transition

Wolfgang Doster

Physics Department E13, Technical University Munich, D-85748 Garching, Germany

ARTICLE INFO

Article history:
Received 30 March 2009
Received in revised form 15 June 2009
Accepted 18 June 2009
Available online 3 July 2009

Keywords:
Protein dynamics
Neutron scattering
Dynamical transition
Glass transition
Mode coupling theory
Protein hydration
Myoglobin
Lysozyme

ABSTRACT

The protein dynamical transition and its connection with the liquid-glass transition (GT) of hydration water and aqueous solvents are reviewed. The protein solvation shell exhibits a regular glass transition, characterized by steps in the specific heat and the thermal expansion coefficient at the calorimetric glass temperature $T_G \approx 170$ K. It implies that the time scale of the structural α-relaxation has reached the experimental time window of 1–100 s. The protein dynamical transition, identified from elastic neutron scattering experiments by enhanced amplitudes of molecular motions exceeding the vibrational level [1], probes the α-process on a shorter time scale. The corresponding liquid-glass transition occurs at higher temperatures, typically 240 K. The GT is generally associated with diverging viscosities, the freezing of long-range translational diffusion in the supercooled liquid. Due to mutual hydrogen bonding, both, protein- and solvent relaxational degrees of freedom slow down in paralled near the GT. However, the freezing of protein motions, where surface-coupled rotational and librational degrees of freedom are arrested, is better characterized as a rubber-glass transition. In contrast, internal protein modes such as the rotation of side chains are not affected. Moreover, ligand binding experiments with myoglobin in various glass-forming solvents show, that only ligand entry and exit rates depend on the local viscosity near the protein surface, but protein-internal ligand migration is not coupled to the solvent. The GT leads to structural arrest on a macroscopic scale due to the microscopic cage effect on the scale of the intermolecular distance. Mode coupling theory provides a theoretical framework to understand the microcopic nature of the GT even in complex systems. The role of the α- and β-process in the dynamics of protein hydration water is evaluated. The protein-solvent GT is triggered by hydrogen bond fluctuations, which give rise to fast β-processes. High-frequency neutron scattering spectra indicate increasing hydrogen bond braking above T_G.

1. Introduction

In structural studies and many commercial applications, proteins are increasingly exposed to low temperatures or solvents at high viscosity. In such systems, the glass transition is an important phenomenon, which has to be accounted for [2]. Protein crystals would not be stable at temperatures far below the freezing point of water without supercooling and the glass transition of crystal water. Experiments with proteins in aqueous solution are restricted to a narrow temperature range. Thus glass-forming solvents, by avoiding crystallization of water, extend the useful temperature range on the low side significantly. This applies not only to structural studies of protein crystals, but in particular to dynamic experiments: the exponential temperature dependence of transition rates allows to discriminate between molecular motions according to their activation energies. Most importantly, such experiments provide insight to dynamic protein–water interactions. This interaction is collective in nature, involving many molecules, which is quite different from local transitions of side chains or methyl groups. The existence of a glass transition is only one of the many consequences, not even the most important one, of collective interactions. Non-exponential relaxation and super-Arrhenius temperature dependence of transition rates are other aspects. The basic mechanism operates on the microscopic scale of the intermolecular distance. It is the cage of nearest neighbours of molecules, which controls the dynamics even on a macroscopic scale. The cage can become a trap, which results in macroscopic structural arrest, when a critical density or temperature is reached. Neutron scattering, providing the relevant spatial- and time resolution, to monitor density fluctuation on a microscopic scale, yields important information on such collective interactions. These interactions are effective even far above the glass temperature in the physiological regime. The glass transition scenario of collective interactions thus involves a wide range of temperatures and time scales and not just the actual glass transition.

The protein dynamical transition was introduced 20 years ago based on neutron scattering experiments with dry and hydrated myoglobin and lysozyme [1]. This topic has been an active field ever since [20,32–36]. But recently, with new experiments, mostly neutron scattering, dielectric relaxation and NMR spectroscopy, the well established view on the subject was challenged, resulting in a deluge of publications [3–6,10–19,21–27]. The question, whether the glass

E-mail addresses: wdoster@ph.tum.de, wolfgang.doster@ph.tum.de.

1570-9639/$ – see front matter © 2009 Elsevier B.V. All rights reserved.
doi:10.1016/j.bbapap.2009.06.019

transition is fragile or strong, a category introduced by Angell, to characterize the curvature in Arrhenius plots, or whether there is some cross-over from fragile to strong behaviour was discussed [13]. A similar "strong" behavior below 220 K was found with dielectric relaxation experiments and was attributed to a secondary relaxation process in amorphous ice [11,14,27]. Some workers deny even the existence of a "transition", claiming that the relaxation times vary smoothly with the temperature [6,11,14,15]. This is however true for any glass transition. It was concluded, that the onset of nonharmonic motion at a particular temperature is not related to a real dynamical transition. Instead it was interpreted as the "trivial" effect of the instrumental resolution function. Moreover, it was questioned, whether the glass transition had any relevance to biological function. A related question was, how a transition detected on a pico-second time scale could affect enzyme activity on the scale of seconds.

A dynamical transition is different from a structural transition. The latter exhibits a sharp transition temperature, which is a thermodynamic time-independent property. The glass transition, in contrast, has a finite width and the effective glass temperature varies with the cooling rate and more generally with the experimental time scale. The time scale of the experiment is thus an essential ingredient of the transition and cannot be ignored. We discussed these features in the context of protein hydration in 1986 [28,29]. Based on infrared experiments, monitoring the protein–water hydrogen bond network, and calorimetric studies, we described a "broad glass transition" of protein hydration water above 170 K. We suggested a distribution of water clusters with different glass temperatures as the main origin of the broadening. Related calorimetric results are presented in this issue. Mechanical relaxation experiments with hydrated protein films by Morozow and Gevorkian also demonstrated the existence of a low temperature glass transition [30]. The term "dynamical transition" instead of glass transition was introduced by us in 1989 [1]. This term comprises the two types of dynamic cross-over, the glass transition, which is quite abrupt and the percolation transition, which is continuous. Both types lead to structural arrest on a macroscopic scale. The question, which concept applies to hydration water, is not yet resolved. Some authors prefer a percolation transition to a glass transition [38,43]. It is also possible, that with decreasing hydration, the glass transition turns into a continuous percolation transition. In the following we argue, that the solvation shell can perform a conventional glass transition, which implies the arrest of translational diffusion within a narrow temperature range. The interaction with the protein however leads to a wider relaxation time distribution and the glass temperature may be different from the bulk phase due changes in solvent composition near the surface. In contrast, protein atoms are localized by covalent bonds and soft interactions, stabilizing the well defined native structure. Thus only rotational and librational degrees of freedom are available, which excludes a regular liquid-glass transition. Since protein motions are "plastisized" by water molecules, one could suggest an analogy to polymer rubbers or elastomers [39]. Stretching of rubbers induces structural relaxation processes, reducing their conformational entropy. The rubber elasticity vanishes, when the structural relaxation time crosses the experimental time window, which defines the rubber-glass transition. The protein elasticity in the native structure can be interpreted as the rubber plateau, which turns into a solid elastic state below the rubber-glass temperature. The plateau terminates at the protein-denaturation temperature, where the structure becomes liquid-like with reduced constraints of protein residues to translational diffusion. Experimental evidence suggests, that the liquid-glass transition of the solvation shell occurs simultaneously with the rubber-glass transition of the protein.

The purpose of the article is to focus on some key questions of the GT and to explain the physical concepts. It is amazing how many misconceptions exist about the glass transition, in particular in the context of proteins [35]. I do not present an exhausting review of the existing literature of the field. To make the point and to illustrate the central ideas I rely mostly on my own experiments. The key questions are: (1) What is the nature of the glass transition, how does it emerge in experiments with biophysical context? (2) What is the biological relevance of the glass transition? (3) What is the nature of the protein-solvent glass transition? (4) Is there a microscopic theory of the glass transition, predicting neutron scattering spectra? (5) What is the role of protein–water hydrogen bonds? Thermal experiments, the step in the specific heat at the glass transition (GT), will be discussed in detail, which is a major point in some articles presented in this issue. I also comment on some models of the GT and protein–water interactions.

2. Basic features of the glass transition

The title of the present article, "the protein-solvent glass transition", emphasizes, that water is not so different in its dynamic interaction with proteins from other glass-forming solvents, like aqueous carbohydrate mixtures. Water is a special liquid, since supercooling is quite difficult in the bulk, but easy to achieve with adsorbed water. About 0.4 g water/g protein are "nonfreezable": roughly two layers of water molecules adsorbed to the protein surface are not incorporated into ice crystals, when the aqueous protein solution freezes. The glass transition is defined by a drastic change in the macroscopic properties of the liquid in the supercooled regime: the shear viscosity diverges abruptly within a narrow temperature range. At the glass temperature T_G, the material undergoes an abrupt transition from a viscous liquid to an amorphous solid [40]. The microscopic structure, expressed by the molecular structure factor $S(q)$, changes smoothly across T_G. The transition always occurs below the melting temperature T_M of the material. Below T_M, the supercooled liquid is not in thermodynamic equilibrium, which would be the crystalline state. It is however still in dynamic equilibrium, since density fluctuations can relax, the corresponding density correlation function decays to zero. The corresponding shear viscosity is finite and the material can flow. At T_G, the system falls out of dynamic equilibrium, where the correlation function decays to a non-zero plateau value and the viscosity increases by more than 10 decades. This happens on a macroscopic time scale, typically 10 to 100 s. Physically, this transition can be classified as the cross-over from ergodic to nonergodic behaviour, which is a fundamental change. Experimentally, a step-like decrease in the specific heat and the thermal expansion coefficient is observed at T_G. At lower temperatures, the degrees of freedom related to density fluctuations appear frozen. This step in the specific heat Δc_P is proportional to the plateau value of the long-time density correlation function, expressing the degree of nonergodicity of the system. The long-time decay thus plays a central role for the macroscopic behaviour. It is associated with the structural relaxation, the α-process, which is the ergodicity-restoring mechanism. The α-relaxation can be measured by a variety of relaxation methods, responding to density fluctuations. One of the most direct ones is dynamic neutron scattering. Dielectric relaxation spectroscopy and D-NMR record the rotational motion of molecules in the liquid. Rotation often involves smaller density fluctuations than translation. The correlation between rotation and the α-relaxation is thus not as tight as with translational degrees of freedom. The α-relaxation time is connected with the shear viscosity of the liquid, η, by the Maxwell equation [41]:

$$\tau_\alpha = G \cdot \eta \tag{1}$$

G denotes the shear modulus of the liquid. The glass transition is thus always linked to the diverging α-relaxation time of the system. This explains, why the glass transition temperature depends on the experimental time scale: a phenomenological definition of the glass temperature sets the experimental time to 100 s, which is equivalent

to a viscosity of 10^{13} Poise. This definition on a scale of seconds is technologically relevant to the processing of liquids near the GT, but has no deep physical meaning. The dynamic nature of the GT can be deduced from the fact that T_G increases with increasing cooling speed. With protein samples, containing more than 0.4 g/g water, the glass temperature and the amount of amorphous ice formed in relation to bulk ice depend on the cooling speed [28,62]. The freezing of liquid protein samples results in freeze concentration of salts, which are not included into the ice crystals. The corresponding pH changes can induce protein denaturation [62]. Experimentally, the GT is observed as a step in the specific heat of the material at the calorimetric glass temperature. Fig. 1 shows an example Δc_P of a 75% glycerol-water solution at T_G. In a conventional scanning calorimeter (DSC), the temperature is changed at constant rate and the required heating power is recorded. The data presented in Fig. 1 were obtained differently, using the method of heat spectroscopy [41,42]. Except for probing a different physical quantity, the method is analogous to dielectric relaxation spectroscopy. The heat spectrometer employs an oscillating heat source, to induce temperature oscillations within the sample at fixed average temperature. The temperature response, its amplitude and phase, depending on the heating frequency, ω_h, and the average temperature, probes the structural relaxation processes. The method yields the spectrum of relaxation times together with the temperature dependence of the average relaxation time, which is given in Fig. 3. The onset at low frequency occurs at the true glass temperature T_G, coincident with DSC results. But with the increasing frequency of the oscillating heat source, the transition shifts to higher temperatures. The effective onset temperature of the GT thus depends on the probe frequency, ω_h. The latter probes, whether the thermal degrees of freedom, expressed by the transient sample temperature, can follow the heating cycle or not. The time scale of the experiment represents thus an essential and non-trivial ingredient of the GT. So far such spectroscopic experiments could be performed only with bulk liquids. With protein-adsorbed water a step in the specific heat around 200 K, shown in Fig. 2, was observed with hydrated myoglobin, myoglobin crystals and with lysozyme in DSC experiments [28,60–63]. Hydrated myoglobin differs from the crystal, since the latter contains ammonium sulfate in addition to 0.35 g/g water. The absolute values of c_P were obtained using calibrated polymer samples and scans within a narrow temperature range. The specific heat of hydration water is larger than for hexagonal ice at low

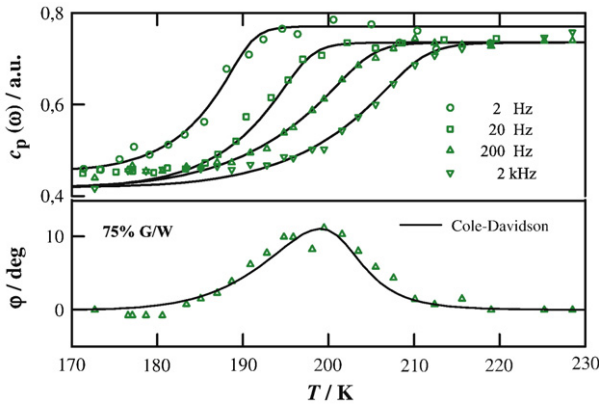

Fig. 1. Specific heat spectroscopy applied to a 75% glycerol-water solution, revealing the α-relaxation in the frequency domain and the glass transition. The frequency-dependent heat has a real part (a) and an absorptive imaginary part (b) similar to the dielectric susceptibility. The sample is heated using an oscillating heat source. The frequency is indicated. The full line is a fit assuming a Cole–Davidson distribution of relaxation times with a stretching parameter of $\beta = 0.5$. Stretched relaxation deviating from a Lorentzian spectrum is a typical feature of the α-process. The resulting temperature dependence of the average relaxation time is shown in Fig. 3. φ denotes the phase shift between heat and temperature oscillations [42].

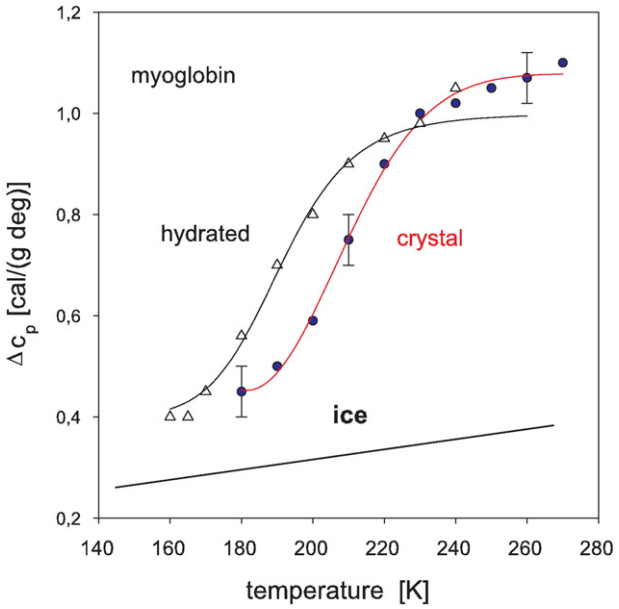

Fig. 2. Specific heat of adsorbed water in hydrated myoglobin powder (0,4 g/g) (triangles) and myoglobin crystals (filled circles) derived from calibrated differential calorimetry experiments. The background of the dry protein was subtracted. The full lines represent fits of Δc_p to the dynamic model as discussed in the text, with Eqs. 2 and 3 [28,29].

temperatures and exceeds the value of bulk water at high temperatures. To visualize the dynamic nature of Δc_P, a simple model of the GT in the protein hydration shell, suggested in 1985 [28,29], is reproduced here: c_P is generally proportional to the thermal degrees of freedom, which are "available" for heat transfer during the experimental time $1/\omega_h = \tau_{exp}$. We thus define the availability function $F(\tau_\alpha, \tau_{exp})$, which is unity, if $\tau_{exp} > \tau_\alpha$ and zero otherwise. For the α-relaxation time we assume an effective Arrhenius law, valid within the narrow temperature range of the transition: $\tau_\alpha = \tau_0 \exp(H/RT)$. H denotes the activation energy and τ_0 is the prefactor. To each degree of freedom an activation energy within a distribution $g(H)$ is assigned. The step Δc_p is then proportional to the following integral:

$$\Delta c_p \propto \int_0^\infty F\left(\tau_{exp}, H\right) g(H) dH \tag{2}$$

We assume for simplicity an exponential decay of $g(H)$ above some minimum enthalpy H_{min}: $g(H) = \exp[-\gamma(H - H_{min})]$ and $g(H < H_{min}) = 0$. γ is the width parameter. H_{min} defines together with τ_{exp} an effective glass temperature T^*_G: $H_{min} = RT^*_G \ln(\tau_{exp}/\tau_0)$. The integration of Eq. 2 yields:

$$\Delta c_p\left(T, \tau_{exp}\right) = \Delta c_p^0\left(1 - \exp\left[-\gamma(T - T^*_G) ln\left(\tau_{exp}/\tau_0\right)\right]\right) \tag{3}$$

which is valid in the range above T^*_G. Δc_P in Fig. 2 with hydrated myoglobin can be adjusted with: $\tau_0 = 10^{-13}$ s, a glass temperature of 180 K at $\tau_{exp} = 1$ s, $H_{min} = 42$ kJ/mol and the width, $\gamma^{-1} \approx 9$ kJ/mol. With τ_{exp}, one changes the availability of thermal degrees of freedom, depending on τ_α. This results in a frequency-dependent specific heat similar to the data shown in Fig. 1. By reducing the experimental time τ_{exp} from 1 s to 10^{-10}s as with neutron back-scattering spectroscopy, one probes the same water α-process on a pico-second time scale. This leads to an upshift of the onset temperature by 70° to 240 K. This continuity in the average structural relaxation time of hydration water is displayed in Fig. 3. Therefore, on a 100 ps time scale the hydration water of myoglobin undergoes its liquid to glass transition at 240 K. A glass is a frozen amorphous solid on the experimental time scales resembling a stop motion picture.

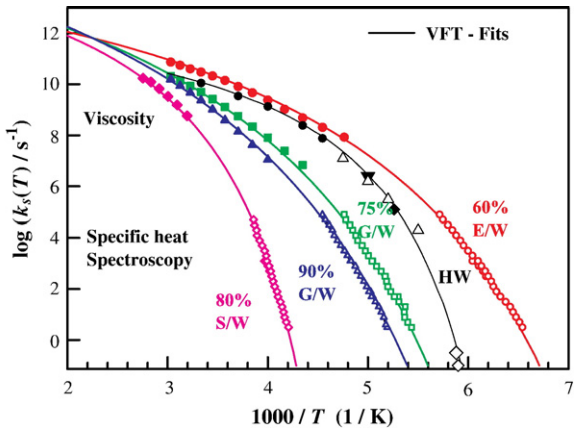

Fig. 3. Arrhenius plot of viscosity and the α-relaxation rate $1/\tau_\alpha = k_S$ of various solvents according to Eq. 1 and data of Fig. 1: 80% sucrose-water (diamonds magenta), 90% glycerol-water (blue triangles), 75% glycerol-water (green squares), 60% ethylen-glycol-water (red circles), HW, hydration water: black circles: myoglobin neutron scattering and calorimetry (open diamond) from Fig. 2 and Ref. [60,63], Mössbauer spectroscopy (top down triangle) [7,32] and dielectric relaxation of myoglobin (open triangles) [11]. The fits to a VFT-equation are also shown (full lines), the parameters are given in Ref. [32,41].

There is a profound difference between the α-relaxation, which is collective in nature and local molecular processes such as rotational transitions of methyl groups. The latter do not couple to the shear viscosity or any other macroscopic property. The methyl group rotation will however, as the α-process, causes a decrease of the elastic intensity in energy-resolved scattering experiments, when the corresponding correlation time overlaps with the resolution function of the spectrometer. This effect will lead to an apparent onset of displacements as observed with hydrated protein samples at 150–180 K with neutron back-scattering [12,32–34]. But this onset has nothing to do with a dynamical transition, which is a collective process. The general increase in motional amplitude, observed for methyl group rotation in proteins with NMR by Lee and Wand [50] is unrelated to the water-coupled dynamical transition. Strikingly, the methyl group rotation in proteins is nearly independent of the protein environment, and is observed even with dry or vitrified proteins [32–35]. Parak et al. interpret the motion of the heme group of myoglobin by a local harmonic potential decorated with traps [56,57]. This view puts the onset of nonharmonic heme displacements in the same class of local molecular motions as the methyl group rotation. Such motions are unrelated to a glass transition. In our own Mössbauer experiments we compared the partially buried heme iron of myoglobin and to ferrocyanide, where the iron is exposed to the solvent. In an 80% sucrose-water solvent nearly identical onset temperatures (250 K) were observed with the two samples. This suggests, that the partially buried heme in myoglobin plays the role of a surface side chain, performing lateral motions in the heme cleft consistent with results obtained with simulations. The heme of myoglobin couples to the solvent via its propionic acid side chains [7]. Moreover, the onset temperature was shown to shift with the viscosity in the solvent near the protein surface as shown in Fig. 7a. The role of the viscosity near the surface, which can be different from the bulk, in relation to the dynamical transition, was discussed here for the first time. Similar observations of shifting anharmonic onsets depending on the solvent were reported later with neutron scattering experiments [58,67]. The viscosity dependence of the anharmonic onset is not only in contrast with the local energy landscape model, but also with the recent proposition, that the dynamical transition originates from viscosity-independent β-processes in the hydration shell [8].

A second important feature, separating glass-generating processes from local molecular motions concerns the coupling to translational diffusion, which is inherently nonlocal. The α-process can be considered as the initial step of translational diffusion on the scale of the intermolecular distance. The macroscopic effect of glass formation is always induced by freezing the translational diffusion in the liquid. Consequently, the glass transition of protein hydration water implies, that translational diffusion has been arrested by strong protein–water hydrogen bonds.

The third feature concerns the temperature dependence of the viscosity or the α-relaxation time. In so-called "fragile" glass-forming liquids the relaxation time shows a super-exponential temperature dependence, the Arrhenius plot appears curved. The apparent barriers thus increase with decreasing temperature. Fig. 3 shows such data of several glass-forming liquids, which have been used in low temperature studies of proteins. It combines measurements of the bulk viscosity and specific heat spectroscopy (Fig. 1) according to Eq. 1. The average relaxation time varies by many orders in magnitude within a small temperature interval. These solvents are well established glass-formers.

In spite of exhibiting a glass transition, $\log(k_S)$ varies continuously with the temperature, there is no abrupt change at any particular temperature. Because of continuous Arrhenius plots, some workers [6,11,14] deny the existence of a dynamical transition all together. One reason is, that the relevant parameters, plotted on a log scale, look smooth even with abrupt changes on a linear scale. The term "transition" implies an abrupt change of a physical quantity within a narrow parameter interval. This interval needs not to be infinitely small as with a phase transition. The experimental width of the GT is always 10 to 20° wide. Moreover, in many applications, a linear plot is more appropriate than a logarithmic scale. For the processing of glass-forming materials it is the abrupt change of thermodynamic quantities within a narrow temperature interval, which is important (Fig. 1). The super-exponential temperature dependence of the α-relaxation rates are often adjusted by the phenomenological Vogel–Fulcher–Tamman law (VFT):

$$k_S = k_0 \exp\left(-T_{vft}/(T - T_0)\right) \tag{4}$$

$k_B\, T_{vft}$ plays the role of a limiting activation energy far away from T_0. The singularity temperature T_0 creates the curvature of the plot, its physical meaning is however unclear. Such fits are shown in Fig. 3, the VFT parameters are given in Ref. [41]. The super-exponential temperature dependence reflects collective behaviour involving strong interactions of many particles and fluctuating barriers. A liquid is not properly represented by a fixed energy landscape. It is thus difficult, to incorporate the solvent within a rigid protein energy landscape. With fluctuating barriers the very concept of a landscape becomes questionable. The α-relaxation time of protein hydration water, determined with neutron scattering of hydrated myoglobin, Mössbauer spectroscopy, dielectric relaxation and thermal experiments is also shown. Water is a highly fragile liquid. Its α-relaxation time can be adjusted to Eq. 4, the extrapolated T_G is close to 170 K, consistent with the calorimetric experiments of Fig. 2. The respective viscosity of adsorbed water ranges between those of 75% glycerol-water and 60% ethylene glycol-water.

3. The relevance of the glass transition to biological function

The notion of "biological function" is somewhat fuzzy. Often some overall process is implied. But the overall reaction is usually composed of various elementary steps. The statement, that lysozyme has no biological function below a critical degree of hydration (0.25 g/g) is to some extent meaningless, since in the absence of the solvent, the exchange and diffusion of substrate molecules are suppressed. Similarly, it was proposed that proteins stop to function below the dynamical transition at 220 K [17]. The counter-proof was given by

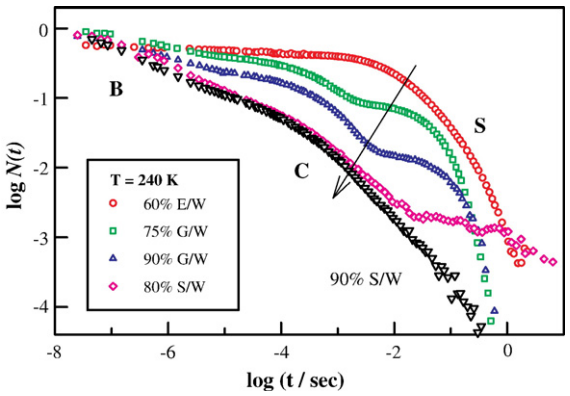

Fig. 4. Kinetics of CO-binding to myoglobin in aqueous solvents (see Fig. 3) with increasing viscosity (arrow) at 240 K. The 90% sucrose-water solvent is a solid glass ($T_G = 310$ K). $N(t)$ denotes the fraction of dissociated CO-molecules after flash photolysis. The decay of three kinetic intermediates B, C and S is indicated. B and C denote internal ligand positions in protein cavities, while S implies ligand binding from the solvent. 'A' denotes the final bound state of CO to the heme iron [41].

Daniel et al. demonstrating enzymic activity at even lower temperatures [21]. Unfortunately, Daniel et al. fell into the trap of a common misconception of the glass transition, which ignores the role of the experimental time window: Protein fluctuations, measured on a pico-second time scale, are compared to enzyme turn over times on a scale of seconds. One year later the same group [22] published a paper on the "time scale dependence" of the dynamical transition. A more detailed account was given in Refs. [24,26]. It is usually overlooked that the relevance of the experimental time scale was already discussed in our early work with myoglobin [1,7,28,29]: The dynamical transition at 240 K was attributed to enhanced resolution of the protein–water α-process by the spectrometer. Smith and Finney even conclude from sub-transition activity that pico-second motions are not relevant to protein function [25]. Myoglobin is not mentioned in their review. Myoglobin is a very well studied protein, which makes it a test case to analyse the physics of protein function and the respective role of dynamics. With flash photolyis experiments, first performed by Frauenfelder and collaborators, one can explore the kinetics of ligand binding and the role of the solvent within a wide range of time scales, temperatures and viscosity. The simple biological function of ligand binding can be decomposed into individual steps, the intermediates are also structurally well known. Early experiments on solvent viscosity effects on the binding kinetics of myoglobin were performed by Beece at al. [48] and Ansari et al. [47]. In these studies all elementary CO-binding rates exhibit some viscosity dependence except the binding to the heme [48]. The respective strength of the protein-solvent coupling was expressed by an exponent $\kappa \leq 1$, connecting the $-\kappa$ kinetic rate of transition $i \rightarrow j$ to the solvent viscosity: $k_{ij} \propto \eta^{-\kappa}$. In the study by Ansari et al. a low-viscosity plateau of the binding rate was invoked. In an extended study of solvent viscosity effects on CO-binding to myoglobin, we could establish, that only the CO-exit and entry rates vary with the solvent viscosity, while internal transfer rates between protein cavities were viscosity-independent [41]. The interpretation of kinetic data strongly depends on the employed kinetic scheme. The branched kinetic scheme of Gibson et al. is now well established: After photolysis from the bound state A, the ligand can move from the geminate position B either to other internal cavities C or to the solvent S: S⇌B⇌C. The bound state communicates with the geminate position B only. Kinetic data at fixed temperature in solvents with increasing viscosity are displayed in Fig. 4 [41]. The data were averaged in real time using a (home-made) log-time recorder. This reduces the noise at long times and low amplitudes. Three kinetic intermediates, characterizing the decay of B, C and S are observed. The various solvents cover a wide range of viscosities (Fig. 3). The 90% sucrose-water solvent is a solid glass at 240 K with $T_G = 310$ K. The main effect of the viscosity increase is a reduction in the amplitude of the slowest process S→A. Its kinetic amplitude defines the escape fraction N_{out} of CO to the solvent. N_{out} decreases with increasing viscosity, because the ligand escape rate decreases, while the rates of internal processes, the exchange between B and C and the formation of the bond with the iron are independent of the solvent. These rates remain finite even in the glassy state at 'infinite" viscosity [41].

Fig. 5 displays the CO-entry rate from the solvent, k_{SB}, versus the viscosity of the bulk solvent. The entry rate is slower than k_S. But their dependence on the temperature is similar, suggesting that $k_{BS} \propto 1/\eta$. A closer inspection reveals a slightly steeper slope of $k_{BS}(T)$ which could be adjusted with a solvent-independent protein barrier of 25 kJ/mol [41]. The sucrose-water system in contrast exhibits a weaker viscosity effect than the bulk. Strikingly, the CO-entry rates in sucrose-water approach the limiting solvent relaxation rate k_S, and would even exceed the solvent rate at higher bulk viscosity. This result makes sense only, if the viscosity near the protein surface is lower than in the bulk. This implies a partial demixing of water and cosolvent near the protein surface. 'Preferential hydration' is known to occur with all carbohydrate-protein solutions, as was shown by Timasheff [46]. The strength of the effect depends on the cosolvent and its partial concentration. In kinetic and dynamic experiments we established, that sucrose at high concentration is strongly excluded from the protein domain [7,41,64]. Preferential protein hydration explains the protein-stabilizing action of aqueous glycerol- and sugar solutions. By contrast, preferential solvation in the case of urea or guanidinium hydrochloride can induce protein denaturation. In conclusion, the physical origin of the apparent fractional viscosity exponent could be either an incorrect kinetic scheme or a lower surface viscosity compared to the bulk. This explanation is however still not accepted by all workers [4,10]. One of the main achievements of Kleinert et al. [41] was to demonstrate the validity of Kramers law of activated escape in the case of ligand entry and exit rates. A 'modified' Kramers law was already invoked by Beece et al. [48] and Ansari et al. [47], but in the latter case no barrier could be detected. Kramers law of activated escape of a particle across a barrier at high damping has the following form [66]:

$$k_{ij} = \frac{\omega_0 \cdot \omega_b}{f} \cdot \exp\left(-H_{ij}/RT\right) \tag{5}$$

ω_0 and ω_b are the frequencies of the harmonic well at the bottom and top of the barrier, respectively. $H_{ij} \gg RT$ denotes the barrier

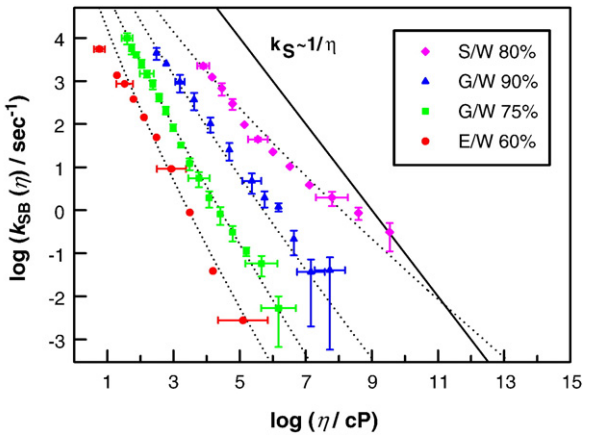

Fig. 5. The entry rate of CO across the surface of myoglobin, k_{SB}, versus bulk viscosity for the solvents introduced in Fig. 3. The the solvent relaxation rate $k_S \propto \eta^{-1}$ (full line) is also shown. The dashed lines represent fits to a Kramers equation, Eq. 5, with a fixed barrier of 24 kJ/mol.

height and f is the friction coefficient in units of inverse seconds. The friction coefficient of a particle in a viscous liquid is proportional to the viscosity and thus the inverse α-relaxation rate: viscosity: $f = \gamma k_S^{-1} \propto \eta_S$. For protein–solvent interactions, η_S denotes the effective viscosity in the vicinity of the protein surface. The dynamic coupling between ligand binding rates and solvent relaxation rates was first discussed in Ref. [42]. Kramers law is thus given by [41]:

$$k_{ij} = \frac{\omega_0 \omega_b k_S}{\gamma} \cdot \exp\left(-H_{ij}/RT\right) \quad (6)$$

The dashed lines in Fig. 5 represent fits to Kramers law (Eq. 6) in the high viscosity limit. Kleinert et al. report a solvent-independent protein barrier of 25 kJ/mol and $\kappa = 1$, for several solvents. The Kramers law, introduced here with k_S as the prefactor, is the basic equation of Frauenfelder's slaving model [4]. However the temperature-dependent barrier term in Eq. 6 was cancelled, yielding $k_{ij} \propto k_S$. This approximation is only correct for moderate protein barriers, provided that the effective activation energies of the solvent are much larger. Moreover, k_S denotes the relaxation rate in the bulk solvent, while, as discussed above, the surface viscosity is the relevant parameter. The slaving relation $k_{SB} \propto k_S$, thus fails in the case of the CO-entry rates to myoglobin in sucrose-water as shown in Fig. 5. The relationship between the ligand entry rate and the solvent relaxation rate reveals the viscous coupling of a Brownian particle, the CO-molecule, to the solvent near the top of the barrier. A viscous coupling of a Brownian particle to its environment is generic to Brownian motion and does not deserve a special name. The ligand entry rate shows a similar viscosity dependence as the exit rate [41].

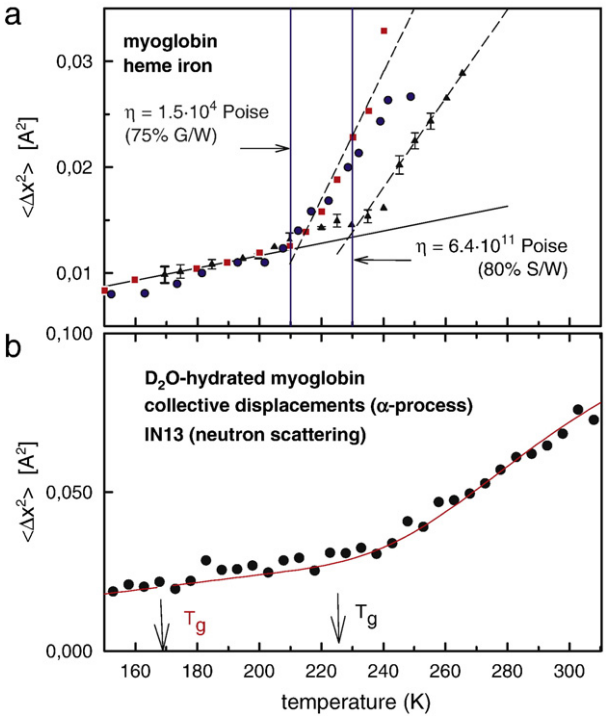

Fig. 7. a) Mean square displacements of the heme iron of myoglobin measured with Mössbauer spectroscopy in various solvents: full circles: water in myoglobin crystals, squares: 75% glycerol-water and triangles: 80% sucrose-water solution. The viscosity at the onset temperatures is indicated. The experimental time scale is 140 ns. b) Mean square displacements of the non-exchangeable hydrogens in D_2O-hydrated myoglobin (0.35 g/g) measured with the back-scattering spectrometer IN13 (ILL). Only the collective Gaussian component is shown, the methyl group contribution was subtracted. The full line is a fit assuming that the α-relaxation water crosses the experimental time window of IN13 [1,32,35]. Instrumental time window: Only processes faster than 50 ps contribute to the displacements.

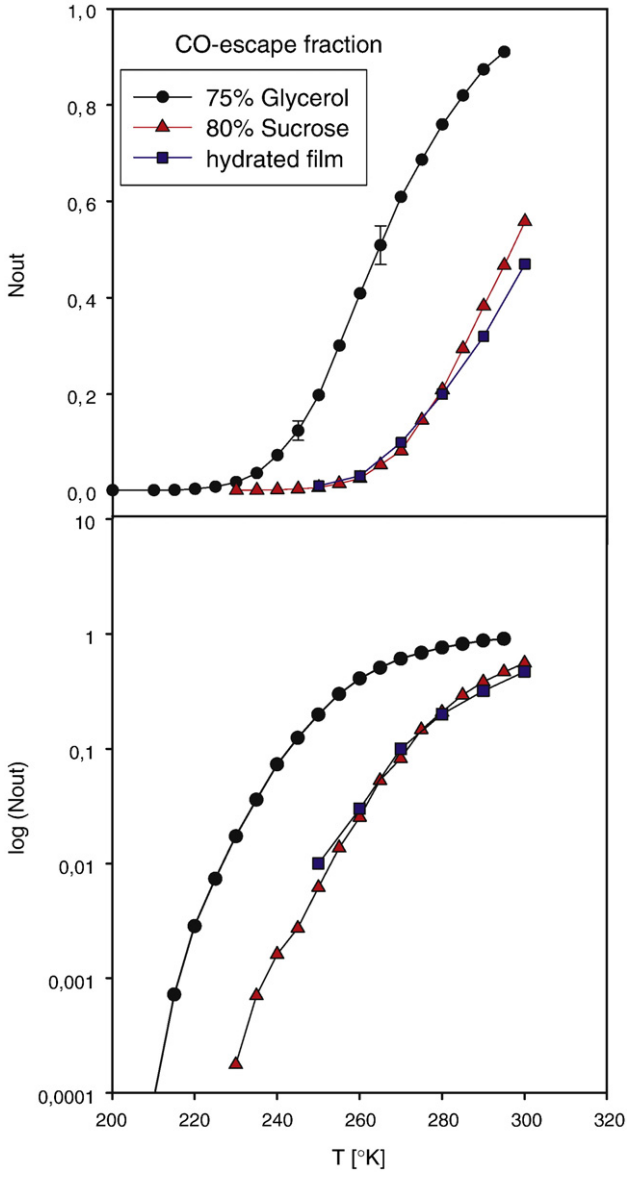

Fig. 6. The fraction of CO-molecules, N_{out}, which move to the solvent after release from the heme iron of myoglobin by flash photolysis. It is derived from the amplitude of the slowest process in Fig. 4 denoted by 'S'. The kinetic data are progressively averaged by a recorder operating on a log-time scale, which enhances the dynamic range in amplitude by four decades. Data obtained with three solvents are shown on a linear scale a) and a log scale b): 75% glycerol-water (circles), 80% sucrose-water (triangles) and a hydrated myoglobin film fabricated with spin-coating (squares).

These experiments were performed with glass-forming solvents. However there is no clear discontinuity visible in the kinetic data induced by the glass transition. In Fig. 6 we display the CO-escape fraction after release at the heme iron versus temperature and for three glass-forming solvents. The same data were plotted either on a linear scale a) or alternatively on a logarithmic scale b). In the latter case N_{out} varies continuously with the temperature, no transition is detected. However on the linear scale one observes a clear onset of ligand escape at 240 K for 75% glycerol-water ($N_{out} \approx 0.1$) and at 270 K with 80% sucrose-water and the hydrated myoglobin film. The onset temperatures are higher than the respective glass temperatures: $T_G = 169$ K (75% glycerol-water) and 228 K for 80% sucrose-water. What is the reason for this discrepancy?

Ligand escape and thus N_{out} are determined by a partitioning between ligand escape and direct rebinding to the heme iron. Thus,

denoting the internal binding rate by k_{BA}, one can approximate the escape fraction N_{out} by [41]:

$$N_{out} = k_{BS}(\eta_S) / (k_{BA} + k_{BS}(\eta_S)). \quad (7)$$

At the onset temperature of 240 K, k_{BA} is approximately $2 \cdot 10^6\ s^{-1}$ and k_{BS} amounts to $2 \cdot 10^5\ s^{-1}$, yielding for $N_{out} = 0.1$. This is about the experimental value of N_{out} at 240 K. In this case, the relevant biological "resolution" time is set by the solvent-independent internal binding rate k_{BA}. Biological function turns on, when the escape rate starts to exceed the internal binding rate. On the kinetic time scale of ligand binding, the "glass transition" occurs at 240 K. The difference to neutron scattering is that the escape rate is only proportional to k_S, while in the case of protein-solvent relaxation the α-process sets the relevant time scale to protein fluctuations directly. A corresponding step in N_{out} was observed in experiments with CO-myoglobin prepared as hydrated films at variable degree of hydration h. N_{out} is zero (on a linear scale) at low hydration and increases above $h = 0.25$ g/g, reaching full level at $h = 0.45$ g/g [31]. The plastisizing action of water is required for ligand exchange, which may apply also to lysozyme and other proteins. The Kramers law of activated escape provides a physically meaningful model accounting for the coupling of protein processes to the solvent: it explains, why the protein rates are approximately, but not exactly proportional to the solvent relaxation rate and the inverse viscosity. It also accounts for the gap between k_{ij} and k_S in terms of a protein barrier and entropic prefactors.

4. Dynamical transition and anharmonic onset of molecular displacements

In this section we briefly establish the connection between the surface viscosity and the anharmonic onset of molecular displacements, observed with Mössbauer spectroscopy and neutron scattering. Fig. 7a shows the displacements of the heme iron of myoglobin in three solvents [7]. Myoglobin crystals and myoglobin in 75% glycerol-water solution exhibit onset temperatures near 200 and 215 K respectively. Crystal water is thus less viscous than 75% glycerol-water, consistent with the results in Fig. 3. The arrows in Fig. 7b indicate the respective glass temperatures of the mixed solvents. The onset temperature in 75% glycerol-water is thus located 40° above T_G. This discrepancy results from the different experimental scale of 1 s (DSC) and 140 ns. The latter is the nuclear lifetime of ^{57}Fe, the isotope used with Mössbauer spectroscopy of the heme group. The viscoelastic relaxation time of the aqueous glycerol solvent has reached 2 μs at 220 K (Fig. 3). It is thus about 10 times larger than the nuclear lifetime of the ^{57}Fe. The onset generally occurs near 5–10 τ_{exp} of the instrument [32]. The onset temperature is thus compatible with a coupling of heme displacements to density fluctuations of the bulk solvent on the same time scale. In 80% sucrose-water the onset temperature has shifted to 230 K [7]. A similar shift was observed for the CO-escape fraction in Fig. 6. This comparison shows, that heme displacements depend on the viscosity of the solvent like the ligand entry and exit rates. The two solvents, glycerol- and sucrose-water, differ mainly in their viscosity at a given temperature. If the bulk viscosity is the essential control variable, one should expect identical viscosities at the respective onset temperatures. The values, given in Fig. 7a, differ however by several orders in magnitude. At 230 K we expect a viscosity near the surface in sucrose-water near 10^4 Poise. Moreover, the glass temperature and the onset temperature nearly coincide in this case, suggesting a common time scale of 1 s, which cannot be correct. These results suggest instead, that the viscosity near the protein surface differs from its bulk value. The same conclusion for 80% sucrose-water was derived from the kinetics of CO-exit and entry rates as shown in Fig. 5.

In Fig. 7b, the displacements of the non-exchangeable protein protons of D_2O-hydrated myoglobin are displayed. We have selected the dynamic component, which is observed only in the hydrated case [35,37]. The onset temperature at 240 K now refers to a different surface viscosity, since we probe the sample on a time scale of 50–100 ps. The onset time should thus be about 1 ns. This is roughly the relaxation time of hydration water at 240 K as Fig. 3 shows. More quantitatively, the full line in Fig. 7b was calculated, assuming that the protein displacements occur exactly on the time scale of hydration water. Input is $\tau_{exp} = 80$ ps of the spectrometer IN13 and the VFT fit to the hydration water relaxation time in Fig. 3. The agreement is quite reasonable, suggesting, that the protein–water α-process consists in a concerted librational motion of protein surface residues, coupled to translational jumps of water molecules on the same time scale. Taken together our experiments demonstrate, that the onset of the dynamical transition depends on the solvent viscosity near the protein surface. This view contrasts with the idea of viscosity-independent β-processes in the hydration shell, controlling the onset of the dynamical transition [8,9].

In recent dielectric relaxation experiments a further slower process was identified, apart from water reorientation, which was assigned to water-coupled protein dynamics [11,14,15]. The protein process displayed a parallel temperature dependence to the water reorientation rates. However, in previous dielectric work by Careri and others, this process was assigned to proton conductivity along the protein–water hydrogen bond network. Proton conductivity naturally depends on water reorientation as a microscopic step and has little in common with protein structural relaxation [43–45].

5. Models of the glass transition

The generic model of the GT is usually illustrated by a particle moving across a rugged energy landscape [40]. Below the GT, the particle is confined in a particular potential well. The disorder of the glass comes about by a set of nearly iso-energetic minima of different structure, which can act as traps. The confinement to a particular trap, depending on the pre-history of cooling, accounts for the nonergodic nature of the glass. Near T_G, the particle can overcome some of the lower barriers, resulting in local "β-processes" in the glass. Well above T_G, also larger barriers are overcome, which gives rise to the collective α-process and long-range diffusion. This popular picture is the basis of Frauenfelder's conformational substate model of protein dynamics [59]. In his article on "energy landscapes and motions in proteins", published in Science in 1991, the solvent was not even mentioned. The rugged energy landscape, non-exponential structural relaxation, the super-Arrhenius temperature dependence of relaxation rates, conformational disorder were all assigned to the protein molecule excluding the solvent. The same "consistent picture" was employed to explain the motion of the heme iron in myoglobin observed with Mössbauer spectroscopy [56]: The heme moves in a rugged harmonic potential, which is decorated with traps. Also the force constant model [68] explains the protein dynamical transition at 180 K, observed with neutron scattering, as detrapping of a particle out of low lying energy states. The nonharmonic onset in these models reflects the enhanced population of excited states and not any time scale. The glass temperature would be a constant, independent of any slow process. In both cases this was shown to be incorrect: The onset temperatures depend on the experimental time scale and the viscosity of the solvent [1,7,58]. The 180 K transition (IN13, $\Delta E = 10$ μeV) occurs at 150 K at higher instrumental resolution (HFBS, $\Delta E = 1$ μeV) [12,32–35].

Of course, in his Science article in 1991, Hans Frauenfelder was probably aware of the important role of the solvent in his experiments, even though it was not mentioned. He had published a paper already in 1980 on solvent viscosity effects in protein dynamics [48]. However, it proved to be difficult to incorporate the solvent into the landscape picture. A liquid cannot be represented by a fixed energy landscape, the barriers due to particle interactions are fluctuating. It is

not the barrier height, which determines the transition rates, but the entropy, associated with the frequency of occurrence of low barrier configurations. These low-density local configurations represent transient holes in the otherwise tightly packed liquid structure. Frauenfelders solution to the problem was to give up, at least partially, the protein energy landscape, and to shift the control entirely to the solvent, which is now "slaving" the protein [4]. In a recent article [8], it was even claimed that 'the image of the protein being essentially passive and being slaved to the environment is not an idle speculation'. Moreover, as in a previous publication [4], our kinetic experiments with myoglobin in viscous solvents [41] are reinterpreted. The internal ligand binding rates, which are independent of the solvent viscosity, are assigned to the control of so-called β-processes in the protein hydration shell. The dynamics of the solvation shell, however, strongly depends on the viscosity near protein surface. This separation into master and slave seems arbitrary, since the protein surface also modifies the structural and dynamic properties of water. Both, water and protein surface are coupled by hydrogen bonds and perform thus correlated motions [1,32]. With neutron scattering a quite powerful tool is available to go beyond simple models.

6. Microscopic theory of the glass transition: mode coupling theory

In 1990, we applied mode coupling theory of liquids to hydrated proteins [55]. This was a courageous attempt, since proteins are very different in structure and dynamic behaviour from liquids. We now believe that the theory should be applied to density fluctuations of the protein hydration shell. Mode coupling theory (MCT) is the only available microscopic theory of liquids. The theory was substantially extended by W. Götze and colleagues to cover the supercooled regime and the liquid to glass transition [51,52,72]. The theory predicts correlation functions and scattering functions of liquid dynamics on a time- and spatial scale relevant to neutron scattering. Therefore a basic understanding of MCT is useful to any biophysicist applying neutron scattering to aqueous systems. MCT assumes, that coupled density fluctuations are controlling the dynamics of the liquid, which leads to a dramatic slowing down of the relevant relaxation times in the supercooled regime. This mechanism of increasing the viscosity by nonlinear coupling of density fluctuations induces structural arrest, when a critical density is reached. The latter is equivalent to a critical temperature T_c, which is easier to measure. Both quantities are independent of the experimental time scale. T_c specifies a true singularity, involving critical fluctuations in contrast to the calorimetric glass temperature or T_0 in Eq. 4.

MCT predicts density correlation functions $\Phi(q,t)$, which are related to the intermediate scattering function $I(q,t)$, observed with neutron scattering. The glass state is distinguished from the liquid by a non-zero nonergodicity parameter $f(q)>0$. $f(q)$ is defined as the long-time value of density correlation function $\Phi(q,t\to\infty)=f(q)$. A non-zero $f(q)$ implies that a complete relaxation of density fluctuations cannot not occur, which is equivalent to saying that the system cannot reach dynamic equilibrium. Spatial heterogeneities can persist. The input of the theory is the static structure factor $S(q)$ of the liquid, which reflects the average structure on the scale of the intermolecular distance. Across the critical temperature T_c, the structure factor $S(q)$ changes smoothly, while a discontinuous change results for the long-time value of the density correlation function from zero if $T>T_c$ to $f(q)=f_q>0$ for $T<T_c$.

Liquids are dense systems, which do not contain channels or holes. Long-range diffusion thus requires a collective rearrangement of many particles. The relevant spatial scale is set by the intermolecular distance, each particle is constrained by a cage of nearest neighbours. Long-range diffusion thus involves the escape out of this cage as an essential initial step of diffusion. This inter-cage transfer is a plausible picture of the α-process, which restores the ergodicity on the respective α-time scale. Above a critical density, the cage becomes a trap and macroscopic structural arrest results. This process is highly nonlinear and is described by an integro-differential equation, the generalized Langevin equation for the density fluctuations [51,72]. It can be visualized as a damped harmonic oscillator equation for the density correlation function $\Phi(q,t)$. The oscillator frequency is denoted by ω_0. The damping has two components, a regular Maxwell friction, γ_0, due to collisions and a relaxing friction kernel $m(\Phi(t))$ which depends again on the density fluctuations:

$$\Phi(q,t) + \omega_0^2\Phi(q,t) + \gamma_0\dot{\Phi}(q,t) + \int_0^t dt' m(t-t')\dot{\Phi}(q,t') = 0 \qquad (8)$$

A general solution to Eq. 8 can be given in the frequency domain for the dynamical structure factor $S(q,\omega)$ [54]:

$$S(q,\omega) = -Im\left\{\frac{\omega + \omega_0^2 M(q,\omega)}{\omega^2 - \omega_0^2 + \omega\omega_0^2 M(q,\omega)}\right\} \qquad (9)$$

'Im' denotes 'imaginary part of' and $i=\sqrt{-1}$. $M(q,\omega)$ represents a generalized friction kernel, which can be decomposed into a Newtonian friction γ_0 (collisions) and a slow relaxing part $m_{ps}(q,\omega)$ due to coupling of density fluctuations:

$$M(q,\omega) = i\gamma/\omega_0^2 + m_{ps}(q,\omega) \qquad (10)$$

In the simplest case of an exponential relaxation of the force correlations, one obtains a Lorentzian friction kernel [54]:

$$m_{ps}(\omega) = -F(q)/(\omega + i/\tau) \qquad (11)$$

Since the density fluctuations are controlled by the time-dependent friction kernel, and the friction kernel depends vice versa on the density fluctuations, a closed system of coupled equations results [51,52,72]. Applications to protein dynamics are given in Ref. [49,54,55]. The predicted relaxation of a supercooled liquid always involves a two-step decay of $\Phi(q,t)$. The initial decay, after vibrational dephasing, describes the intra-cage local dynamics, which has been termed the fast β-process. The second step is the main structural relaxation, the α-process of moving out of the cage. Several scaling laws describing the time and temperature dependence of the α- and β-relaxation time were deduced [51]. This is illustrated in Fig. 8 for an ideal glass transition of a hard sphere system. The parameter is the density or the volume fraction, the critical value is $\phi=0.52$. At temperatures well below the critical temperature T_c, which is generally above T_G, the fast β-process decays to a plateau at a fixed rate. But the respective amplitude decreases with decreasing temperature (not shown, see below). At T_c, the local β-amplitude has reached a critical value, where the plateau starts to decay via the α-process at long times. Increasing the temperature is speeding up the α-process until it merges with the β-process at high temperatures. Fast local and slower collective processes are characteristic of condensed matter dynamics. They appear not only in neutron scattering spectra of liquids but also in those of polymers and proteins. In our initial publication on the dynamical transition, we calculated the intermediate scattering function of hydrated myoglobin, which also showed these two components [1]. Moreover, the dynamic susceptibilities of hydrated myoglobin displayed some features predicted for liquids by MCT. This was confirmed by a quantitative analysis, a T_c of 194 K was derived [55]. However, protein atoms are localized and cannot assume a liquid state, which is defined by long-range translational diffusion. MCT should thus be applied to the hydration water, while the protein performs a correlated rubber-glass transition. The reason, why neutron scattering spectra of hydrated proteins seem to have much in common with liquids is their dynamic interaction with the solvent. Thus water molecules and

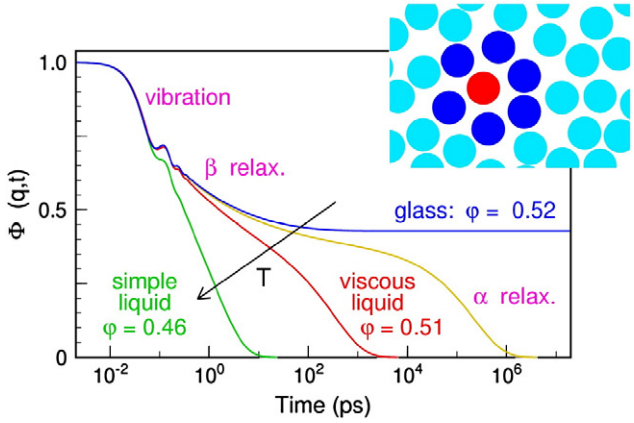

Fig. 8. Schematic plot of the density correlation function $\Phi(q,t)$ of a hard sphere liquid across the glass transition as predicted by MCT. The essential parameter is the volume fraction ϕ or the temperature. The time range of the α- and β-process is indicated [51,52].

protein residues perform correlated motions on the same time scale at short times, which is the α-process. We have published time-resolved mean square displacement to demonstrate this fact [32].

Fig. 9 shows the intermediate scattering function of adsorbed water for myoglobin at $h=0.34$ g/g. $I(q,t)$ displays the two-step decay as a function of the temperature, resembling the MCT-calculations of Fig. 8. The characteristic time of the fast β-process remains fixed with temperature, only its amplitude decreases, when approaching the glassy state. This is a characteristic feature of intra-cavity fluctuations, where only the amplitude changes with the density. With water, the cage formed by the nearest neighbours involves not only van der Waals interactions but also hydrogen bonds. Intra-cage fluctuations are thus associated with opening and closing hydrogen bonds. By this mechanism, a nonharmonic onset in the displacements, observed with neutron scattering, would reflect a critical fraction of open bonds. This was our initial idea of the first transition observed near 180 K. The second transition observed at 240 K was attributed to the second process, the α-relaxation, moving into the resolution window of the back-scattering spectrometer IN13 [1]. However, to discriminate these fast fluctuations from slower methyl group rotations, the latter dominate in the back-scattering window above 180 K, one has to employ time-of-flight spectroscopy [35,37]. The second process, the α-relaxation, determines the viscosity near the protein surface. The slowing down of the density fluctuations with decreasing temperature is striking. The plateau at 180 K indicates structural arrest of the protein surface. $I(q,t)$ exhibits a stretched relaxation, which is properly fitted by a Kohlrausch function: $I(q,t)=\exp\{-(t/\tau)^{\beta}\}$. The resulting stretching exponent of 0.5 is common for glass-forming liquids. The α-relaxation rates diverge super-exponentially as shown in Fig. 3. The adjusted VFT plot extrapolates to $T_G=170$ K. The q-dependence of $I(q,t)$ is consistent with translational displacements and the nonlocal nature of this process [32,49]. MCT can be used to fit the time-resolved mean square displacements derived from neutron scattering experiment with myoglobin hydration water [49]. For a hard sphere liquid MCT predicts the following short-time expansion [53]:

$$1/3\langle\Delta x^2\rangle = r_s^2 + \delta^2(t/\tau)^b + O\left[(t/\tau)^{2b}\right] \quad (12)$$

The parameters are linked to the cage size, the effective hard cord diameter, $a\approx 2.6$ Å, in the case of water: $r_s\approx a/9$ and $\delta\approx a/6$ [53]. τ denotes the α-relaxation time and "b" is the stretching exponent. Fig. 10 compares experimental data, time-resolved squared displacements for water adsorbed to hydrated myoglobin, myoglobin residues (D_2O-hydrated) and for dehydrated myoglobin with Eq. (12). The initial free flight is interrupted by collisions with the nearest neighbours, the cage effect reveals itself as an intermediate plateau. For longer times, the displacements increase again due to inter-cage motion. For water, we derive parameters, which are consistent with a hard core diameter of 2.6 Å, at 300 K. The correlation time is $\tau=15\pm2$ ps and the stretching exponent of $b=0.6$ is lower than $b=1$ expected for regular Gaussian diffusion. This approach is theoretically better justified than the model of water diffusion inside a sphere [65].

The protein residues exhibit a much smaller cage size of 1.3 Å. However in the D_2O-hydrated case we derive $\tau=18\pm3$ ps, which is nearly identical with the water relaxation time. This result indicates again, that the displacements of water and protein residues are correlated on a pico-second time scale, although their absolute amplitudes differ. For the dry sample, the relaxation time is much larger, about 50 ps.

Only mode coupling theory can provide a clear definition of α- and β-processes. The β-process is defined as local intra-cage relaxation, which is always faster than the structural reorganisation of the cage. Below we assign the fast water β-relaxation to hydrogen bond

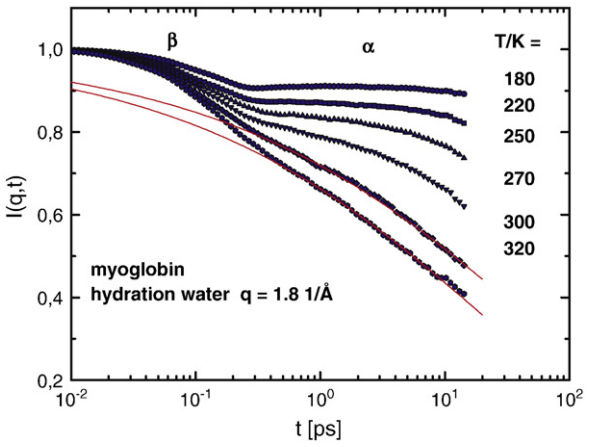

Fig. 9. Intermediate scattering function $I(q,t)$ of myoglobin hydration water derived by Fourier transforming H_2O/D_2O difference spectra (IN6, ILL) to the time domain. The time range of the α- and β processes are indicated. With decreasing temperature the α-process slows down. The time scale of the fast β-process is nearly independent of the temperature, only the amplitude decreases at low temperatures, compare to Fig. 8. [49].

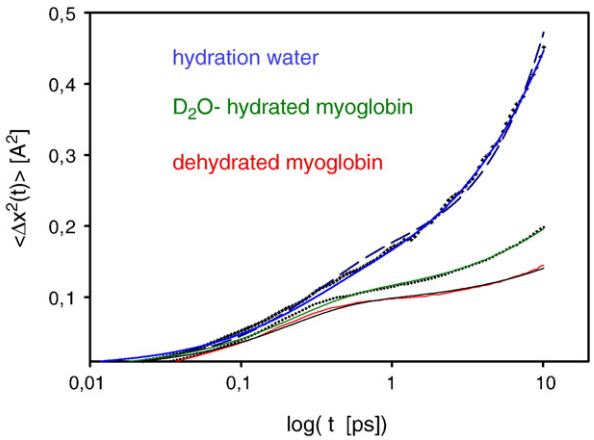

Fig. 10. Time-resolved mean square displacements of water adsorbed to myoglobin at 0.34 g/g, the non-exchangeable protons of hydrated myoglobin (D_2O-hydrated) and for dry myoglobin. The data were derived based on a model-independent moment analysis of the intermediate scattering function (Fig. 9) as described in Ref. [32,33,49]. The full lines are fits to the MCT equation12 with parameters given in the text. The dashed line assumes regular diffusion or $b=1$.

fluctuations in the dihedral molecular arrangement. In the literature the term β-process is used for all kinds of secondary processes, which differ in their temperature dependence from the primary relaxation. A unique functional role of β-processes (instead of the α-process) in the protein hydration shell was recently postulated by Frauenfelder et al. [6,8,9]. β-processes are observed however in the glassy state at low temperatures [11,27]. Their molecular nature is unclear, a possible scenario is the diffusion of Bjerrum defects in amorphous ice.

7. Mechanism of the dynamical transition

The MCT equations can be solved for simple systems explicitly, such as hard sphere liquids. But they provide a general framework to unravel the mechanism of the glass transition also in complex systems. One reason is, that the influence of the repulsive part of the molecular potential is often more important than specific attractive forces, provided that long-range interactions are quenched. The basic mechanism of the GT is the cage effect, operating on the scale of the intermolecular distance. Thus, the macroscopic effect of turning a liquid into a solid, results from structural arrest on a microscopic scale. The first step is thus to understand the properties of the cage. The constraints imposed on a water molecule by the cage of nearest neighbours are dominated by a network of hydrogen bonds in a tetrahedral arrangement. Thus, the fastest process, the β-relaxation, may be assigned to displacements of a water molecule inside the cage due to hydrogen bond fluctuations. This suggests, that the amplitude of the β-process in Fig. 9 increasing with the temperature reflects enhanced local structural fluctuations. This process can be considered as the precursor of the main structural relaxation, which requires the disintegration of the cage. The fluctuations between open and closed can be modelled with two states of different energy. The down-barrier to closing the bond is quite small and thus rate-limiting, implying a large and nearly temperature-independent β-relaxation rate. The population of open bonds however increases exponentially with the temperature. This model was used to account for the anharmonic onset in the displacements at 180 K observed with neutron scattering [1]. The asymmetric two-state model was considered as the mechanism of triggering the dynamical transition in the sense of a particle moving out of a trap. The EISF of this process suggested instead rotational jumps of side chains. The main contribution results from methyl group rotation, a molecular process unrelated to the glass transition, which interferes however with water-coupled motions in the back-scattering energy window [32–34]. Instead, the fast β-process emerges in the low resolution, high intensity time-of-flight spectrometer [37]. In 1989 [1,55], we already noticed, that the high-frequency TOF-relaxation spectrum of hydrated myoglobin exhibits a constant linewidth, but its amplitude would increase exponentially with the temperature. This effect was assigned to a changing population of open hydrogen bonds [37]. The mechanism of bond braking is dominated by rotational librations of water molecules. The far-IR spectrum of water exhibits a strong hindered rotation band near 80 meV (640 cm^{-1}). Fig. 11 displays the high-frequency spectra of adsorbed H_2O, corrected for protein contributions as observed with inelastic neutron scattering. Such spectra were first shown in Ref. [49]. The hindered rotation band of myoglobin hydration water broadens significantly with increasing temperature. The broadening of the high-frequency vibrational band at 80 meV goes in parallel with an increase in amplitude of the high-frequency relaxation spectrum near 2 meV, which is the β-regime. This suggests, that the relaxation amplitude of local motions is directly connected to rotational oscillations, which lead to barrier crossing. Molecular dynamic simulations of hydrated proteins also established the important role of hydrogen bond fluctuations to fast protein and water dynamics [18,19].

In the case of hydration water, a significant fraction of the bonds are formed with amide groups (NH and C=O) or polar side chains of the protein. The 400 water molecules in a myoglobin crystal are engaged

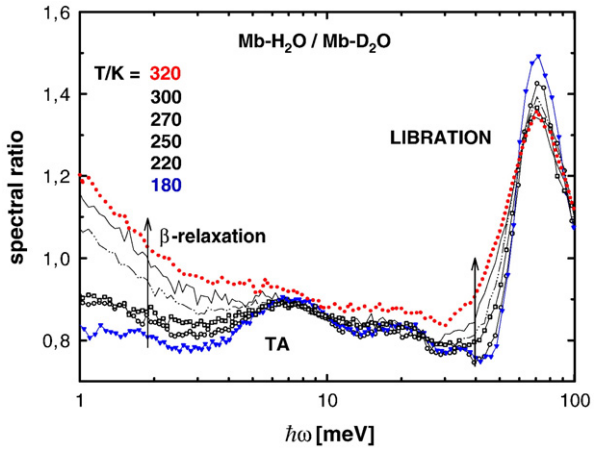

Fig. 11. High-frequency water spectra of hydrated myoglobin (0.34 g/g), Mb-H_2O corrected for the protein contribution by Mb-D_2O at fixed angle θ [49]. The hindered rotation band (libration) and a translational band TA are indicated. The arrows point towards increasing temperature. Also the relaxational β-regime is marked by an arrow. Its spectral amplitude increases exponentially with the temperature, suggesting a population change between two states of different energy. The experiments were performed with the instrument IN6 at the ILL in Grenoble.

in ca. 1600 hydrogen bonds, one quarter of it or 400 bonds involve polar protein residues [69,70]. The minority fraction of protein–water bonds may explain, why the high-frequency spectrum of hydration water, the translational and librational bands are almost identical with those of bulk water [49]. It also explains, why adsorbed water is not "bound" to the protein surface, but can perform translational diffusion as required for a liquid. This was shown in Refs. 32 and 49. Some time ago, we studied the infrared spectrum of the O–H(D) stretching vibration of protein-adsorbed water as a function of the temperature, degree of hydration and cosolvent concentration [28,29]. We also investigated these effects on the amide I and II absorption bands of myoglobin and lysozyme [64]. The uncoupled O–D stretch as well as the amide bands are sensitive to the average hydrogen bond length. The anharmonicity of the H-bond network yields the dominating contribution to the thermal expansion coefficient. Thus by recording the central frequency of the O–D stretching vibration, one can estimate the thermal expansion coefficient, as it turns out, almost in quantitative agreement with volumetric measurements [64]. The protein–water hydrogen bonds are generally stronger than water–water bonds. In all cases with hydration water and glass-forming solvents, we observed a discontinuous change in the thermal expansion coefficient at the calorimetric glass temperature T_G. Fig. 12 shows the corresponding step of the linear expansion coefficient at 170 K, the glass temperature of the adsorbed water. A similar step occurs for glycerol. For comparison, we also show the elastic scattering intensity for H_2O-hydrated D-phycocyanin, reflecting water dynamics. The measurements were performed with back-scattering spectroscopy at a resolution of 1 μeV, implying an effective experimental time of 600–700 ps. The onset of the transition in the elastic intensity occurs at 220 K, which is compatible with calculations assuming that the α-relaxation time of water enters the time window of the spectrometer. The time-temperature shift of 50° is thus compatible with the α-process, which reaches the time scale of seconds at 170 K. Thus a critical number of open bonds controlled by the β-process is a prerequisite for the α-relaxation to occur. For water, an inter-cage displacement becomes possible only, if four hydrogen bonds are simultaneously broken.

8. Conclusions

The protein-solvent glass transition scenario describes the low temperature or high viscosity properties of solvated proteins. The

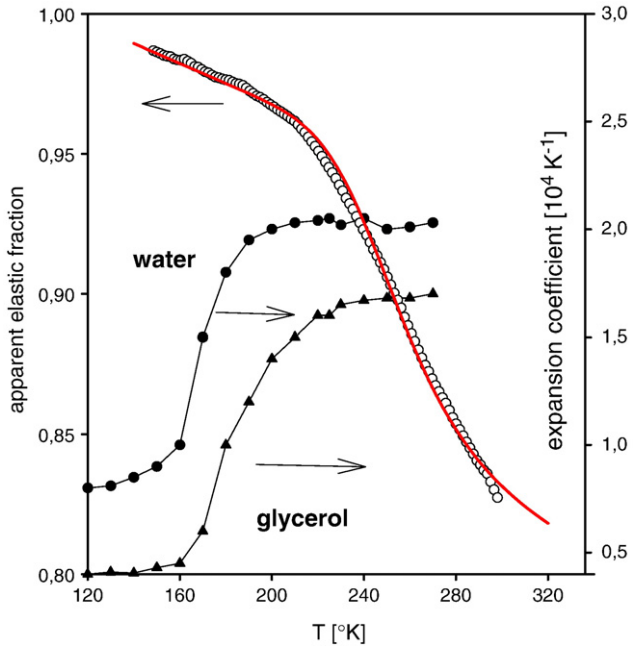

Fig. 12. Linear thermal expansion coefficients, derived from the near infrared O–D stretching absorption spectrum of hydrated myoglobin (0.34 g/g, black dots) and of glycerol (triangles) [28,64]. Open circles: Elastic fraction of H_2O-hydrated D-phycocyanin (0.3 g/g) determined with neutron back-scattering (SPHERES, FRM 2). The full line is calculated, assuming, that the α-process of hydration water, shifting into the frequency window of the spectrometer, causes the decrease in the elastic intensity.

transition occurs, when the main structural relaxation of the protein solvation shell crosses the time scale defined by the experiment: As a result, the density correlation functions decay to a non-zero plateau, as in Fig. 9, which is a nonergodic state: Solvent-coupled structural fluctuations appear arrested. The complexity of the GT derives from the fact, that it unifies fast and slow, collective and local processes simultaneously: It leads to macroscopic changes, the transition from a liquid to a solid, based on the cage effect, operating on a microscopic scale. Mode coupling theory provides a theoretical framework to interpret neutron scattering spectra even at physiological temperatures far away from T_G. The effective glass temperature varies for a particular system, depending on the experimental time scale and the cooling rate. The transition is thus not linked to a particular temperature, but concerns collective protein-solvent coupling within a wide range of time and temperature. The transition in the physical parameters appears discontinuous on a linear scale, but looks continuous on a log scale. In many applications though, a linear scale is more appropriate. This applies for instance to the mean square displacements of atoms in proteins. The GT affects the function of myoglobin by reducing the ligand entry and exit rates, while internal processes near the active site remain active.

The recent interest and revival of the protein glass transition is focused on the temperature range near T_G, well below the physiologically relevant regime. In this issue, Sokolov, Swenson and collaborators conclude that the protein–water α-process observed with neutron scattering is different from the one causing the thermal effects at 170 K. New local processes emerge below 200 K due to the specific properties of amorphous ice, as was shown with dielectric relaxation spectroscopy and NMR [11,27]. The relaxation scenario of hydration water at 170 K may thus be different from the one observed at 240 K. This does not invalidate the GT concept, which is generally applied to biofunctional processes above 200 K. Moreover these new features are observed with methods, which are sensitive to molecular reorientation. In contrast, the α-process always involves inter-cage translation. The neutron scattering experiments, shown in Fig. 9, reflect the translation of water and do not show any anomaly down to 180 K. Figs. 3 and 12 also reveal a continuum of α-relaxation times: The discontinouities in the thermal expansion of the hydrogen bond network and the specific heat of water further support the conventional picture of a glass transition. Angell's idea of postulating β-processes instead of an α-relaxation in hydrated proteins was based on the missing thermal signal in his homopeptide experiments [5]. Homopeptides are different from proteins and a thermal transition in the hydration shell of myoglobin had been reported already at that time [28]. Mode coupling theory predicts that the anomalies of supercooled liquids become evident near a critical temperature T_c, which is located well above the conventional T_G. Their analysis requires fast methods like neutron scattering to study the fluctuations of the hydrogen bond network. In this sense, understanding protein dynamics implies as a prerequisite to unravel the unusual properties of adsorbed water. The protein surface is known to act as a structure breaker of the dihedral arrangement, which may destroy the anomalous fluctuations observed with bulk water. This could have implications on the conjectured second critical point. So far there is no convincing demonstration of a structural change in the hydration shell near 210 K, which could explain the observed apparent fragile to strong transition in the α-relaxation temperature dependence [13]. The transition in the elastic intensity, shown in Fig. 12, can be fully assigned to a conventional glass transition on a 600 ps time scale without invoking a structural change. It is a unique feature of the glass transition that both sides, liquid and glass, differ very little in structure. In the future, the structural fluctuations in the protein solvation shell, well above T_G, will be further investigated to reveal collective relaxation of functional degrees of freedom. The effect of the specific protein structure on such processes also needs further study [71].

Acknowledgement

This work was supported by a grant of the Deutsche Forschungsgemeinschaft, SFB 533 on Light-induced dynamics in biopolymers. Technical support by the Institut Laue-Langevin in Grenoble, France, is gratefully acknowledged.

References

[1] W. Doster, S. Cusack, W. Petry, Dynamical transition of myoglobin revealed by inelastic neutron scattering, Nature 337 (1989) 754–756.
[2] L. Slade, H. Levin, J.W. Finley, in: J.W. Finley, R.D. Philips (Eds.), Protein quality and the effects of processing, Marcel Dekker, 1989, pp. 9–121.
[3] H. Frauenfelder, P.W. Fenimore, B.H. McMahon, Hydration, slaving and protein function, Biophys. Chem. 98 (2002) 35–48.
[4] P.W. Fenimore, H. Frauenfelder, B.H. McMahon, F.G. Parak, Slaving: solvent fluctuation dominate protein dynamics and functions, PNAS 99 (2002) 16047–16051.
[5] J.L. Green, J. Fan, C.A. Angell, The protein-glass analogy: some insights from homopeptide comparisons, Phys. Chem. 98 (1994) 13780–13790.
[6] P.W. Fenimore, H. Frauenfelder, B.H. McMahon, B. Young, Bulk-solvent and hydration-shell fluctuations control protein motions and functions, Proc. Natl. Acad. Sci. U. S. A. 10 (2004) 14408–14412.
[7] H. Lichtengegger, W. Doster, Th. Kleinert, A. Birk, B. Sepiol, G. Vogl, Heme-solvent coupling, a Mössbauer study of myoglobin in sucrose, Biophys. J. 76 (1999) 414–422.
[8] H. Frauenfelder, G. Chen, J. Berendsen, P.W. Fenimore, H. Jansson, B.H. McMahon, I.R. Stroe, J. Swenson, R.D. Young, A unified model of protein dynamics, Proc. Natl. Acad. Sci. 106 (2009) 5129–5134.
[9] G. Chen, P.W. Fenimore, H. Frauenfelder, F. Mezei, J. Swenson, R.D. Young, Protein fluctuations explored by inelastic neutron scattering and dielectric relaxation spectroscopy, Phil. Mag. 88 (2008) 3877–3883.
[10] H. Frauenfelder, P.W. Fenimore, G. Chen, B.H. McMahon, Protein folding is slaved to solvent motions, PNAS 103 (2006) 15469–15472.
[11] J. Swenson, H. Jansson, R. Bergman, Relaxation processes in super-cooled and confined water and implications for protein dynamics, Phys. Rev. Lett. 96 (2006) 247802–247804.
[12] R.H. Roh, V.N. Novikov, R.B. Gregory, J.E. Curtis, Z. Chowduri, A.P. Sokolov, Onset of unharmonicity in protein dynamics, Phys. Rev. Lett. 95 (2005) 038101–038103.
[13] S.H. Chen, L. Liu, E. Fratini, P. Baglioni, A. Farone, E. Mamontov, Observation of fragile-strong dynamic cross-over in protein hydration water, PNAS USA 103 (2008) 9012–9016.

[14] S. Khodadi, S. Pawlus, A.P. Sokolov, Influence of hydration on protein dynamics, combining dielectric and neutron scattering spectroscopy data, J. Phys. Chem. B 112 (2008) 14273–14280.
[15] S. Khodadadi, J.H. Roh, V.G. Sakai, E. Mamontov, A.P. Sokolov, The origin of the dynamic transition in proteins, J. Chem. Phys. 128 (2008) 1951061–1951065.
[16] K.L. Nai, S. Capaccioli, N. Shinyashiki, The protein glass transition and the role of the solvent, J. Phys. B. 112 (2) (2008) 3826–3832.
[17] D. Ringe, G.A. Petsko, The glass transition in protein dynamics: why it occurs and how to exploit it, Biophys. Chem. 104 (2003) 667–680.
[18] M. Tarek, D. Tobias, Single particle and collective dynamics of protein hydration water, Phys. Rev. Lett. 89 (2002) 13801–13804.
[19] M. Tarek, D. Tobias, The role of protein–water hydrogen bonds in the dynamical transition of proteins, Phys. Rev. Lett. 88 (2002) 381011–381013.
[20] F. Gabel, D. Bicout, U. Lehnert, M. Tehei, M. Weik, G. Zaccai, Protein dynamics, studied by neutron scattering, Qu. Rev. Biophys. 35 (2002) 1.
[21] D. Daniel, J. Smith, M. Ferrand, S. Henry, R.J. Dunn, J.L. Finney, Enzyme activity below the dynamical transition, Biophys. J. 75 (1998) 2504–2507.
[22] R.M. Daniel, J.L. Finney, V. Reat, R. Dunn, M. Ferrand, J. Smith, Enzyme dynamics and activity, the time scale dependence of dynamical transitions, Biophys. J. 77 (1999) 2184–2219.
[23] A.L. Tournier, J.C. Smith, Principal components of the protein dynamical transition, Phys. Rev. Lett. 91 (20) (2003) 208106-1–208106-4.
[24] T. Becker, J. Smith, Energy resolution and dynamical heterogeneity effects on elastic incoherent neutron scattering from molecular systems, Phys. Rev. E 67 (2003) 021904-1–021904-8.
[25] R.M. Daniel, R.V. Dunn, J.L. Finney, J.C. Smith, The role of dynamics in enzyme activity, Ann. Rev. Biophys. Biomol. Struc. 32 (2003) 3269–3292.
[26] T. Becker, J.A. Hayward, J.L. Finney, R.M. Daniel, J. Smith, Neutron frequency windows and the protein dynamical transition, Biophys. J. 87 (2004) 1436–1444.
[27] M. Vogel, Origins of apparent fragile-to-strong transitions of protein hydration waters, Phys. Rev. Lett. 101 (2008) 255701–255704.
[28] W. Doster, E. Lüscher, A. Bachleitner, R. Dunau, M. Hiebl, Thermal properties of water in myoglobin crystals and solutions at subzero temperatures, Biophys. J. 50 (1986) 213–219.
[29] W. Doster, Glass transition of hydration water and structural flexibility of myoglobin, in: A. Eherenberg, R. Rigler, A. Gräslund, L. Nilssson (Eds.), Structure, Dynamics and Function of Biomolecues, Springer Series in Biophysics, Vol. 1, 1986, pp. 34–38.
[30] V.N. Morozov, S. Gevorkian, Low temperature glass transition in proteins, Biopol. 24 (1985) 1785–1799.
[31] W. Doster, Th. Kleinert, M. Settles and F. Post, Hydration effects on protein function, Water Biomolecule Interaction Conference, Proceedings of the Italian Physical Society 43 (1993) 127–130, Bologna, Ed. M.U. Palma, M.B. Palma-Vitorelli and F. Parak.
[32] W. Doster, M. Settles, Protein–water displacement distributions, Biochim. Biophys. Act. 1749 (2005) 173–186.
[33] W. Doster, Brownian oscillator analysis of molecular motions in biomolecules, in: J. Fitter, T. Gutberlet, J. Katsaras (Eds.), Neutron Scattering in Biology, Springer Series Biological and Medical Physics, Biomedical Engeneering, 2005, pp. 461–482.
[34] W. Doster, Dynamic structural distibutions in proteins, Physica B 385–386 (2006) 831–834.
[35] W. Doster, The dynamical transition of proteins, concepts and misconceptions, Eur. Biophys. J. 37 (2008) 591–602.
[36] M. Ferrand, A. Dianoux, W. Petry, G. Zaccai, Thermal motions and function of bacteriorhodopsin in purple membranes: effects of temperature and hydration studied by neutron scattering, Proc. Natl. Acad. Sci. U. S. A. 90 (1993) 9668–9672.
[37] W. Doster and M. Settles, Dynamical transition of proteins, the role of hydrogen bonds: in Hydration Processes in Biology (1998) p.177–190 (Les Houches Lectures) Ed. Marie-Claire Bellissent-Funel, IOS Press.
[38] I. Brovchenko, A. Krukau, N. Smolin, A. Oleinikova, A. Geiger, R. Winter, Thermal breaking in spanning water networks in the hydration shells of proteins, J. Chem. Phys. 123 (2005) 224905–224909.
[39] R.H. Austin, D.L. Stein, J. Wang, Terbium luminescence-lifetime heterogeneity and protein equilibrium conformational dynamics, Proc. Natl. Acad. Sci. U. S. A. 84 (1987) 1541–1545.
[40] J. Wong, A.C. Angell, Glass Structure by Spectroscopy, Marcel Dekker, 1976.
[41] Th. Kleinert, W. Doster, H. Leyser, W. Petry, V. Schwarz, M. Settles, Solvent composition and viscosity effects on the kinetics of CO-binding to horse myoglobin, Biochem. 37 (1998) 717–733.
[42] M. Settles, W. Doster, A. Schulte and F. Post Specific heat spectroscopy of dynamic protein-solvent interactions Biophys. Chem. 43 (1992) 107–116.
[43] M. Settles, W. Doster, F. Kremer, F. Post, W. Schirmacher, Percolation approach to proton conductivity in hydrated protein powders, Phil. Mag. B 65 (1992) 861–866.
[44] G. Careri, A. Ginsanti, J.A. Rupley, Percolation transition of proton conductivity of hydrated protein powders, Proc. Natl. Acad. Sci. U. S. A. 82 (1985) 5342.
[45] J.J. Hawkes, R. Pethig, Biochim. Biophys. Act. 952 (1988) 27.
[46] S.N. Timasheff, Protein hydration, thermodynamic binding and preferential hydration, Biochem. 19 (2002) 13473–13482.
[47] A. Ansari, C. Jones, E.R. Henry, J. Hofrichter, M.A. Eaton, The role of solvent viscosity in the dynamics of protein conformational changes, Science 256 (1992) 1796–1799.
[48] D. Beece, L. Eisenstein, H. Frauenfelder, D. Good, M. Marden, L. Reinisch, A. Reynolds, L. Sorenson, K. Yu, Viscosity and protein dynamics, Biochem. 19 (1980) 5147–5162.
[49] M. Settles, W. Doster, Anomalous diffusion of protein hydration water, Faraday Discussion 103 (1996) 302–2963.
[50] A.L. Lee, J. Wand, Microscopic origins of entropy, heat capacity and the glass transition in proteins, Nature 411 (2001) 501–504.
[51] W. Götze, L. Sjögren, Relaxation processes in supercooled liquids, Rep. Prog. Phys. 55 (1992) 241–376.
[52] W. Götze, L. Sjögren, Comments on the mode coupling theory for structural relaxation, Chem. Phys. 212 (1996) 47–59.
[53] M. Fuchs, I. Hofacker, A. Latz, Mode coupling theory of the hard core liquid, Phys. Rev. A. 45 (1992) 898–902.
[54] H. Leyser, W. Doster, M. Diehl, Far infrared emission by Boson peak vibrations of a globular protein, Phys. Rev. Lett. 14 (1999) 2987–2991.
[55] W. Doster, S. Cusack, W. Petry, Dynamic instability of liquid-like motions in proteins, Phys. Rev. Lett. 65 (1990) 1083–1086.
[56] F. Parak, E.W. Knapp, A consistent picture of protein dynamics, Proc. Natl. Acad. Sci. U. S. A. 81 (1984) 7088–7092.
[57] F. Parak, K. Achterhold, Protein dynamics on different timescales, J. Phys. Chem. Solids 66 (2005) 2257–2262.
[58] A.M. Tsai, D.A. Neumann, L.N. Bell, Molecular dynamics of solid-state lysozyme as affected by glycerol and water, a neutron scattering study, Biophys. J. 79 (2000) 2728–2732.
[59] H. Frauenfelder, S. Sligar, P. Wolynes, The energy landscapes and motions of proteins, Science 254 (1991) 1598–1602.
[60] Y. Miyazaki, T. Matsuo, H. Suga, Glass transition of myoglobin crystal, Chem. Phys. Lett. 213 (1993) 303–305.
[61] Y. Miyasaki, T. Matsuo, H. Suga, Low temperature heat capacity and glassy behaviour of lyozyme crystal, J. Phys. Chem. B 104 (2000) 8044–8050.
[62] G. Sartor, E. Mayer, G.P. Johari, Calorimetric studies of the kinetic unfreezing of molecular motions in hydrated lysozyme, hemoglobin and myoglobin, Biophys. J. 66 (1994) 249–258.
[63] K. Kawai, T. Suzuki, M. Oguni, Low temperature glass transitions of quenched and annealed bovine serum albumin solutions, Biophys. J. 90 (2006) 3732–3738.
[64] F. Demmel, W. Doster, W. Petry, A. Schulte, Vibrational frequencies as a probe of hydrogen bonds: thermal expansion and glass transition of myoglobin in mixed solvents, Europ. Biophys. J. 26 (1997) 327–335.
[65] M.C. Bellissent-Funel, J. Teixera, K.F. Bradley, S.H. Chen, H.L. Crespi, Single particle dynamics of hydration water in protein, Physica B 180–181 (1992) 740–744.
[66] H.A. Kramers, Physica 7 (1940) 284.
[67] V. Reat, R. Dunn, M. Ferrand, J.L. Finney, R.M. Daniel, J.C. Smith, Solvent dependence of dynamic transitions in protein solutions, Proc. Natl. Acad. Sci. U. S. A. 97 (2000) 9961–9966.
[68] J. Zaccai, How soft is a protein? A protein force constant measured by neutron scattering, Science 288 (2000) 1604–1607.
[69] E.N. Baker, R.E. Hubbard, Hydrogen bonding in globular proteins, Prog. Biophys. Molec. Biol. 44 (1984) 98–180.
[70] X. Cheng, B. Schönborn, Hydration in protein crystals, Acta Cryst. B 46 (1990) 195–201.
[71] A. Gaspar, M.S. Appavou, S. Busch, T. Unruh, W. Doster, Dynamics of well folded and natively disordered proteins in solution, a time of flight neutron scattering study, Eur. Biophys. J. 37 (2008) 573–580.
[72] W. Götze, Complex dynamics of glass-forming liquids, International Series of Monographs on Physics 143, Oxford Science Publications, (2009).